

DESY PRC R&D 03/04  
PROJECT: DSTAR-TRIG  
TYPE OF DOCUMENT: EOI

**Phase I: A Proposal for R&D Work on a Trigger  
for  $D^{*\pm} \rightarrow D^0\pi^\pm \rightarrow h_1^+h_2^-\pi^\pm$  Decays Using the  
*HERA-B* Detector**

**Phase II: An Experiment to Study  $CP$  Violation  
and Mixing in the  $D^0-\overline{D}^0$  System via  
 $D^0 \rightarrow K^+\pi^-/K^+K^-/\pi^+\pi^-$  Decays**

A. J. Schwartz

University of Cincinnati, Cincinnati, Ohio 45221 USA

**2 October 2003**

Corresponding Author: A. Schwartz, [schwartz@fnal.gov](mailto:schwartz@fnal.gov)

**Abstract**

We propose to initiate R&D to develop and test a  $D^{*\pm} \rightarrow D^0\pi^\pm$  trigger that would operate with the *HERA-B* detector. We estimate that the *HERA-B* detector running with such a trigger would reconstruct large, competitive tagged samples of singly-Cabibbo-suppressed  $D^0 \rightarrow K^+K^-$ ,  $D^0 \rightarrow \pi^+\pi^-$ , and doubly-Cabibbo-suppressed  $D^0 \rightarrow K^+\pi^-$  decays. The decay-time distributions of these samples would be used to measure/constrain mixing and  $CP$ -violating effects in the  $D^0-\overline{D}^0$  system with high sensitivity. If the R & D project was successful and a  $D^*$  trigger demonstrated, a strong case could be made for a follow-on charm mixing/ $CP$  experiment.

# 1 Introduction

The *HERA-B* experimental program has been completed, and the detector is in principle available for other physics experiments. We study here the feasibility of using the detector to record a large sample of two-body  $D^0 \rightarrow h_1^+ h_2^-$  decays and precisely reconstruct their decay-time distributions. These decays would be triggered on via  $D^{*+} \rightarrow D^0 \pi^+$  and  $D^{*-} \rightarrow \bar{D}^0 \pi^-$  decays, and thus the flavor of the  $D^0$  or  $\bar{D}^0$  would be identified with a high-quality tag. Such samples would be used to measure:

- the ratio of lifetimes for  $D^0 \rightarrow K^+ K^-$  and  $D^0 \rightarrow K^- \pi^+$  decays<sup>1</sup>, which can be used to measure/constrain the mixing parameter  $y$ ;
- the time distribution of doubly-Cabibbo-suppressed  $D^0 \rightarrow K^+ \pi^-$  decays, which can be used to measure/constrain the mixing parameters  $x'$  and  $y'$ ;
- by comparing the lifetime distributions of  $D^0 \rightarrow K^+ K^- / \pi^+ \pi^-$  with that for  $\bar{D}^0 \rightarrow K^+ K^- / \pi^+ \pi^-$ , one would search for  $CP$  violation in the  $D^0$ - $\bar{D}^0$  system.
- by comparing the lifetime distributions of  $D^0 \rightarrow K^+ \pi^-$  decays with that for  $\bar{D}^0 \rightarrow K^- \pi^+$ , one would also search for  $CP$  violation in the  $D^0$ - $\bar{D}^0$  system. As this final state is doubly-Cabibbo-suppressed, the partial width is especially sensitive to non-Standard-Model physics.

The method of measuring the mixing parameter  $y \equiv \Delta\Gamma/(2\Gamma)$  was originally used by E791 [1] and the FOCUS [2] experiment. The latter result was  $(3.42 \pm 1.39 \pm 0.74)\%$ , which differs from zero by 2.2 standard deviations and generated much interest. Since then the method has been used by both Belle (with  $158 \text{ fb}^{-1}$ ) and BaBar (with  $91 \text{ fb}^{-1}$ ); the results are  $(1.15 \pm 0.69 \pm 0.38)\%$  [3] and  $(0.8 \pm 0.4^{+0.5}_{-0.4})\%$  [4], respectively. It is interesting to note that all three experiments measure a positive value for  $y$ .

The method of measuring  $x'$  and  $y'$  by measuring the time distribution of  $D^0 \rightarrow K^+ \pi^-$  decays has been used by FNAL E791 [5], CLEO [6], and Babar [7]. A similar analysis is now underway at Belle [8]. The best limits (from Babar using  $57.1 \text{ fb}^{-1}$  of data) are  $x'^2 < 0.0022$  and  $-0.056 < y' < 0.039$  at 95% C.L. A related analysis of  $D^0 \rightarrow K^+ \pi^-$  decays by the FOCUS experiment obtains a constraining relationship among  $x'$ ,  $y'$ , and the ratio of  $D^0 \rightarrow K^+ \pi^-$  to  $D^0 \rightarrow K^- \pi^+$  decay rates [9].

The CDF experiment [10] may not have sufficient  $\pi/K$  discrimination to separate the much rarer  $D^0 \rightarrow K^+ \pi^-$  decays from  $D^0 \rightarrow K^- \pi^+$ , as misidentifying the tracks still gives a two-body invariant mass close to  $m_{D^0}$ . The SVD track-trigger that CDF uses to record charm decays is efficient only for  $p_T \gtrsim 2 \text{ GeV}/c$ ; for this momentum range, the time-of-flight system is not useful and all particle identification derives from  $dE/dx$  measurement in the central tracking chamber. The CLEO-c [11] experiment produces  $D^0$  mesons almost at rest, and thus they do not measure decay-time information directly.

Given the current (and future) BaBar and Belle results, the question is: would a measurement made with the *HERA-B* detector and a  $D^{*+} \rightarrow D^0 \pi^+$  trigger be competitive? Note that these measurements play to the strengths of the *HERA-B* detector: the large Lorentz boost and silicon-based vertex detector result in excellent vertex and decay time

---

<sup>1</sup>Throughout this document, charge-conjugate modes are implicitly included unless noted otherwise.

resolution, and the RICH detector provides very good  $\pi/K$  discrimination. The latter is necessary to reject large backgrounds originating from Cabibbo-favored  $D^0 \rightarrow K^-\pi^+$  decays.

In this proposal we study the sensitivity of the *HERA-B* detector to  $D^0$ - $\bar{D}^0$  mixing in doubly-Cabibbo-suppressed (DCS)  $D^0 \rightarrow K^+\pi^-$  decays. These decays would be recorded by a  $D^{*+} \rightarrow D^0\pi^+$  trigger along with the singly-Cabibbo-suppressed (SCS) decays  $D^0 \rightarrow K^+K^-$  and  $D^0 \rightarrow \pi^+\pi^-$ . Due to lack of time we have not separately studied the latter channels. The detector acceptance and efficiencies are calculated via Monte Carlo simulation; the rejection rate of a  $D^{*+} \rightarrow D^0\pi^+$  trigger is calculated by studying minimum bias data recorded in December 2002. We find the precision obtainable by *HERA-B* to be competitive with and possibly better than that of the  $e^+e^-$  experiments. A measurement of mixing in the  $D^0$ - $\bar{D}^0$  system could be a first indication of new physics, and observing  $CP$  violation would be strong evidence of physics beyond the Standard Model. For a recent review, see Ref. [12].

The technique that would allow *HERA-B* to record such a data sample is a trigger for  $D^{*+} \rightarrow D^0\pi^+$  decays. In the following sections we describe the design of this trigger and its expected performance. To proceed with an experiment based on such a trigger, more development work and testing would need to be done. Thus, we divide this proposal into two phases: the first phase is that of a trigger R & D project, and the second phase is that of an actual experimental data run with the goal of recording very large samples of tagged  $D^0 \rightarrow K^+K^-$ ,  $D^0 \rightarrow \pi^+\pi^-$ , and  $D^0 \rightarrow K^+\pi^-$  decays. Clearly the feasibility of phase II depends on what is learned during phase I; if the trigger concept can be demonstrated to work, then a strong physics case could be made to proceed with phase II. At this point in time we are requesting consideration only of phase I.

The proposal is organized as follows: in Sec. 2 we give an overview of the mixing/ $CP$  measurements to provide some background. In Sec. 3 we describe how the  $D^*$  trigger would operate and calculate the rejection factor for minimum bias events. In Sec. 4 we calculate the nominal acceptance and trigger efficiency for  $D^0 \rightarrow K^+\pi^-$  decays, and in Sec. 5 we calculate the expected  $D^0 \rightarrow K^+K^-$ ,  $D^0 \rightarrow \pi^+\pi^-$ , and  $D^0 \rightarrow K^+\pi^-$  sample sizes. In Sec. 6 we use the  $D^0 \rightarrow K^+\pi^-$  sample size to estimate the precision to which the experiment could measure the mixing parameters  $x'$  and  $y'$ . Finally, in Sec. 7 we present the proposed plan for the R & D phase of the project and the resources needed.

## 2 Experimental Method

As mentioned above, the *HERA-B* detector would record a large sample of  $D^0 \rightarrow h_1^+h_2^-$  decays by triggering on  $D^{*+} \rightarrow D^0\pi^+$ ,  $D^0 \rightarrow h_1^+h_2^-$  decays. This decay chain has two advantages:

- the charge of the pion originating from the  $D^*$  identifies whether the accompanying meson is  $D^0$  or  $\bar{D}^0$ , and thus the resultant sample is flavor-tagged;
- it greatly reduces background as the mass difference between the  $D^{*+}$  and  $D^0 + \pi^+$  final state is very small – only  $5.9 \text{ MeV}/c^2$ .

The first feature allows measurement of  $CP$ -violating effects in  $D^0$  decays, while the second feature makes a  $D^*$  trigger possible in a hadroproduction environment. At  $HERA-B$  center-of-mass energies, more than half of  $D^0$  mesons originate from  $D^{*+} \rightarrow D^0 \pi^+$  decays.

To measure the mixing parameter  $y$  one compares the lifetime distribution of  $D^0 \rightarrow K^+ K^-$  or  $D^0 \rightarrow \pi^+ \pi^-$  decays with that of  $D^0 \rightarrow K^- \pi^+$  decays. The  $K^+ K^-$  final state is  $CP = +1$  and, assuming no  $CP$  violation in  $D^0$ - $\bar{D}^0$  mixing, the lifetime distribution is  $\propto e^{-\Gamma_1 t}$ . The  $K^- \pi^+$  final state is an equal admixture of  $CP = +1$  and  $CP = -1$  and thus its lifetime distribution is essentially  $e^{-(\Gamma_1 + \Gamma_2)t/2}$ . Thus,  $y \equiv \Delta\Gamma/(2\bar{\Gamma}) = (\Gamma_1 - \Gamma_2)/(\Gamma_1 + \Gamma_2) = \Gamma_{KK}/\Gamma_{K\pi} - 1$ .

To measure the mixing parameters  $x'$  and  $y'$  via  $D^0 \rightarrow K^+ \pi^-$  decays, one plots the lifetime distribution. This decay receives contributions from both a doubly-Cabibbo-suppressed amplitude and a “mixing” amplitude  $D^0 \rightarrow \bar{D}^0 \rightarrow K^+ \pi^-$ ; as the amplitudes have different decay time dependences, their relative contributions can be unfolded from the decay time distribution. This distribution is often parametrized as:

$$\frac{dN_{K^+\pi^-}}{dt} \propto \left[ R + \sqrt{R} y' \left( \frac{t}{\tau} \right) + \frac{1}{4} (x'^2 + y'^2) \left( \frac{t}{\tau} \right)^2 \right] e^{-t/\tau}, \quad (1)$$

where  $R = \Gamma(D^0 \rightarrow K^+ \pi^-)/\Gamma(D^0 \rightarrow K^- \pi^+)$ ,  $x' = x \cos \delta + y \sin \delta$ ,  $y' = y \cos \delta - x \sin \delta$ ,  $x = \Delta m/\Gamma$ ,  $y = \Delta\Gamma/2\Gamma$ , and  $\delta$  is the strong phase difference between the doubly-Cabibbo-suppressed amplitude and the Cabibbo-favored amplitude. The fundamental mixing parameters are  $x$  and  $y$ , whereas the “rotated” parameters  $x'$  and  $y'$  are what one measures. (Note that the  $\tau_{K\pi}/\tau_{KK} - 1$  measurement discussed above yields  $y$ , and by comparing with  $y'$  one determines the strong phase difference  $\delta$ .) In Eq. (1), the first term in brackets results from the doubly-Cabibbo-suppressed amplitude, the last term from the mixed amplitude, and the middle term from the interference between the two. To illustrate this, the individual contributions of the three terms for one choice of  $x'$  and  $y'$  are plotted in Fig. 1. Thus, one fits the time-dependence of the wrong-sign (WS) sample to Eq. (1) to extract the parameters  $R$ ,  $x'^2$ , and  $y'$ .

One would search for  $CP$  violation in  $D^0 \rightarrow h_1^+ h_2^-$  decays in two ways: separately fitting the lifetime distributions of  $D^0 \rightarrow K^+ K^-/\pi^+ \pi^-$  and  $\bar{D}^0 \rightarrow K^+ K^-/\pi^+ \pi^-$  decays and comparing; and separately fitting the lifetime distributions of  $D^0 \rightarrow K^+ \pi^-$  and  $\bar{D}^0 \rightarrow K^- \pi^+$  decays and comparing. In the latter case one would obtain the six results  $R_+$ ,  $x'_+$ ,  $y'_+$ ,  $R_-$ ,  $x'_-$ , and  $y'_-$ , and construct the  $CP$  observables  $R_{CP} = (R_+ - R_-)/(R_+ + R_-)$ ,  $x'_{CP} = (x'_+ - x'_-)/(x'_+ + x'_-)$ , and  $y'_{CP} = (y'_+ - y'_-)/(y'_+ + y'_-)$ .  $CP$  violation in general arises from three sources: (a) unequal mixing between  $D^0$  and  $\bar{D}^0$ , (b) interference between a mixed amplitude and an unmixed amplitude (e.g., as in  $B^0 \rightarrow J/\psi K_S^0$ ), and (c) interference between two unmixed amplitudes (e.g., “penguin” and tree amplitudes, referred to as “direct”  $CP$  violation). These effects manifest themselves in  $D^0 \rightarrow K^+ K^-/\pi^+ \pi^-$  and  $D^0 \rightarrow K^+ \pi^-$  in different ways; e.g., direct  $CP$  violation can enter these modes with different strengths [12]. Thus it is important to search for  $CP$ -violating effects in all three channels.

It should be noted that to measure small  $CP$  asymmetries, any charge bias in the detector acceptance must be understood. To measure this one would use Cabibbo-favored  $D^0 \rightarrow K^- \pi^+$  decays, which would be produced and triggered on in large quantities; i.e., one

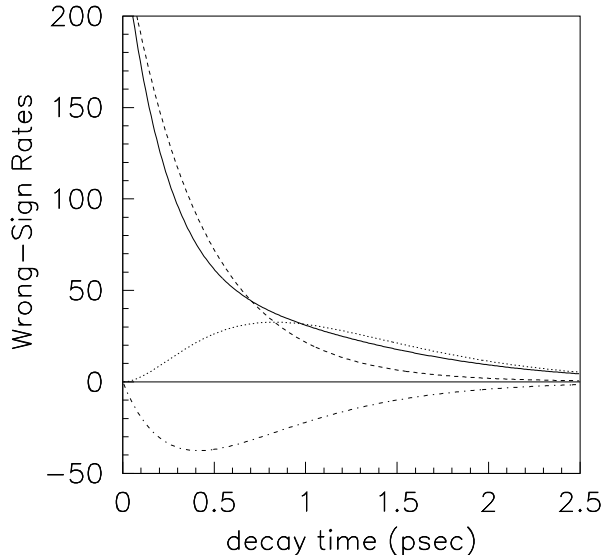


Figure 1: The contribution to the lifetime distribution resulting from the doubly-Cabibbo-suppressed amplitude (dashed curve), the mixed amplitude (dotted curve), and the interference between the two (dotted-dashed curve). The overall time dependence is plotted as the solid curve.

would compare the lifetime distribution of  $D^0 \rightarrow K^- \pi^+$  decays with that of  $\bar{D}^0 \rightarrow K^+ \pi^-$ . As this decay mode should not exhibit any  $CP$  violation, any difference observed in the lifetime distributions could be used to correct the  $K^+ K^- / \pi^+ \pi^-$  and DCS  $D^0 \rightarrow K^+ \pi^-$  lifetime distributions.

### 3 Trigger Scheme and Rejection

To record  $D^0 \rightarrow h^+ h^-$  decays, the *HERA-B* detector must trigger on kaons and pions. This objective is quite different from that of the original *HERA-B* trigger, which was designed to trigger on  $B^0 \rightarrow J/\psi K_S^0$  decays. Nonetheless, the basic operational steps are the same: finding and reconstructing tracks, and selecting events based on momentum and mass criteria. Most of the existing FLT hardware can be used without modification to trigger on  $D^0 \rightarrow h_1^+ h_2^-$  decays. However, to trigger on hadrons the FLT must use pretrigger seeds generated by the high- $p_T$  (HPT) pretrigger system, rather than by the MUON and ECAL pretrigger systems. To obtain sufficient rejection of minimum bias events, the trigger will exploit an unusual kinematic feature of  $D^{*+} \rightarrow D^0 \pi^+$  decays: that the mass difference  $m_{D^*} - m_{D^0} - m_\pi$  is only  $5.9 \text{ MeV}/c^2$ . There are two kinematic consequences of this:

1. since the  $D^0$  and  $\pi^+$  resulting from the  $D^{*+}$  have very small momentum in the  $D^{*+}$  rest frame, the ratio of their momenta in the lab frame is  $\gamma(p_{D^0}^* + \beta E_{D^0}^*) / \gamma(p_\pi^* + \beta E_\pi^*) \approx \gamma \beta E_{D^0}^* / \gamma \beta E_\pi^* \approx m_{D^0} / m_\pi$ , where  $p^*$  and  $E^*$  are quantities in the  $D^*$  rest frame. This ratio is large:  $1.865/0.139 = 13.4$ .

- conservation of 4-momentum dictates  $P_\pi + P_{D^0} = P_{D^*}$ . Squaring both sides gives  $2P_\pi \cdot P_{D^0} = m_{D^*}^2 - m_\pi^2 - m_{D^0}^2 = 0.544 \text{ (GeV}/c^2)^2$ , or  $P_\pi \cdot P_{D^0} = 0.272 \text{ (GeV}/c^2)^2$ . This is a relatively small value.

In principle, the FLT has enough tracking information available to select events based on the momentum ratio  $p_{D^0}/p_\pi$  and the dot-product  $P_\pi \cdot P_{D^0}$ . In the next section we study the rejection of these cuts using real data: minimum bias events recording during the December 2002 minimum bias run.

### 3.1 FLT Trigger

The objective is to find a set of requirements the FLT is capable of making that provides enough rejection to satisfy the SLT input bandwidth. For this study we assume this bandwidth to be 50 kHz; thus, to run at an interaction rate of 1 MHz would require an FLT rejection factor of 20.

We have obtained this rejection factor with the following requirements. All information utilized is available to the FLT; i.e., only RSEG's found in the PC chambers are used, and their momenta are obtained via the formula:

$$\frac{q}{p} \approx - \frac{(x - z \cdot \theta_x) \sqrt{1 + \theta_x^2}}{(2200 \cdot 0.00029975 \cdot 450) \sqrt{1 + \theta_x^2 + \theta_y^2}}, \quad (2)$$

where  $x, z, \theta_x \equiv dx/dz$ , and  $\theta_y \equiv dy/dz$  are evaluated at PC1. The expression in parenthesis in the denominator is  $\int B d\ell$  in units of  $\text{GeV}/c$ . We subsequently require that:

- there be two RSEG's in the PC chambers with opposite charge. Both RSEG's must traverse all four PC chambers and also be accepted by either all three iHPT chambers or all three oHPT chambers.
- the RSEG's must satisfy the momentum asymmetry requirement  $|p_A - p_B| / (p_A + p_B) < 0.70$ .
- the RSEGs must have a  $K\pi$  invariant mass satisfying  $1.82 < m_{K\pi} < 2.01 \text{ GeV}/c^2$ . Since the FLT does not have PID information, this requirement is tested with both daughters assumed to be the kaon; if either combination passes the cut, the event is passed. The RSEG corresponding to the successful kaon candidate must be accepted by TC1; this ensures that the kaon traverses the RICH.
- there must be a third RSEG in the PC chambers that traverses all four PC chambers and is accepted by either all three iHPT chambers or all three oHPT chambers.
- this third RSEG together with the first two RSEGs must satisfy the momentum ratio cut  $10 < p_{rat} < 19 \text{ GeV}/c$ , where  $p_{rat} = (p_{z(1)} + p_{z(2)}) / p_{z(3)}$ .
- the third RSEG together with the first two RSEGs must satisfy the "dot-product cut"  $P_3 \cdot (P_1 + P_2) < 0.32$ , where  $P_1, P_2, P_3$  are 4-vectors.

The rejection obtained by each of these requirements is listed in Table 1. The overall rejection factor is 20, the amount needed.

	$N$	Fraction	
		relative	absolute
Events read	10000	1.	1.
2 RSEGs in PC region, both accepted by iHPT or oHPT, ( $q_1 \cdot q_2$ ) = -1, $ p_{asym}  < 0.70$	6812	0.681	0.681
kaon accepted by TC1	6703	0.984	0.670
$1.820 < m_{K\pi} < 2.010$ GeV/ $c^2$	1837	0.274	0.184
$10.0 < p_{rat} < 19.0$	1538	0.837	0.154
$p_{dot} < 0.32$	526	0.342	0.053
$\pi_s$ : $ x_{swm}  < 18$ cm, $ y_{swm}  < 18$ cm	378	0.719	0.719
$ m_{K\pi} - m_{D^0}  < 100$ MeV/ $c^2$ (RTRA)	108	0.286	0.205
$10 < p_{rat} < 19$ (RTRA)	98	0.907	0.186
$p_{dot} < 0.32$ (RTRA)	84	0.857	0.160

Table 1: The number of minimum bias events passing FLT-level selection requirements (top half), and SLT/4LT-level requirements (bottom half).

Fig. 2 shows plots of  $p_{asym}$ ,  $m_{K\pi}$ ,  $p_{rat}$ , and  $p_{dot}$  obtained from minimum bias events and calculated using only RSEG (PC) information. The events entering each plot have passed previous requirements in the order listed in Table 1. The  $m_{K\pi}$  distribution exhibits an enhancement near  $m_{D^0}$  due to the two possible choices made for the kaon track; the selection window used is asymmetric with respect to  $m_{D^0}$  because that characteristic is observed in Monte Carlo signal events.

### 3.2 SLT and Higher-Level Triggers

The SLT, working together with the TLT/4LT, must reduce this event rate further. As the maximum event logging rate is  $\sim 200$  Hz, the rejection factor needed is nominally  $50\,000/200 = 250$ . Fortunately, there is much information available to the SLT/4LT to accomplish this: track segments in the VDS that can be used to calculate impact parameters with respect to the target wires; RICH information for identifying the kaon; and a magnetic field map with which to swim/refit tracks, resulting in superior momentum resolution than that obtained via Eq. (2). Of these possible requirements we have studied the following:

- swimming the RSEG corresponding to the  $\pi_s$  upstream through the magnet to the position of the target wires ( $z = 0$ ) and checking whether the resultant  $(x, y)$  position is within some nominal distance from the wires. The cut studied here is  $|x| < 18$  cm,  $|y| < 18$  cm.
- making the mass cut  $|m_{K\pi} - m_{D^0}| < 100$  MeV/ $c^2$  using RTRA quantities;
- making the ratio cut  $10.0 < p_{rat} < 19.0$  using RTRA quantities and the swum RSEG momenta for the  $\pi_s$  candidate;
- making the dot-product cut  $p_{dot} < 0.32$  using RTRA quantities and the swum RSEG momenta for the  $\pi_s$  candidate.

The rejection factors of these cuts are listed also in Table 1; the overall rejection factor is 6.3. Thus, an additional factor of 40 is needed. However, the DAQ system can potentially be upgraded to increase the maximum logging rate to  $\sim 1$  kHz, and in this case only an additional rejection factor of 8 is needed. Such a factor was obtained by the impact parameter trigger employed by the SELEX experiment at FNAL. This trigger recorded  $D^0 \rightarrow K^- \pi^+$ ,  $D^0 \rightarrow K^- \pi^+ \pi^- \pi^+$ ,  $D^+ / D_s^+ \rightarrow K^- K^+ \pi^+$ , and  $\Lambda_c^+ / \Xi_c^+ \rightarrow p K^- \pi^+$  decays in (mostly)  $\Sigma^- N$  interactions; the beam energy was 600 GeV. The trigger algorithm reconstructed tracks in downstream PWC chambers, extrapolated the tracks upstream into a silicon strip vertex detector, and used hits found in the vertex detector to reconstruct “silicon tracks.” These tracks (along with the beam track) were fit to a primary vertex. If the fit had an acceptable  $\chi^2$  and used all tracks, then the event was rejected as “non-charm”. If the fit had a large  $\chi^2$ , i.e., one or more tracks were inconsistent with originating from a common vertex, then the event was kept. The trigger ran in a 17-processor SGI Challenge computer with an input rate of 4 kHz. It achieved a minimum bias rejection factor of 8 and was about 50% efficient for a typical charm signal decay.

We thus assume that the requisite SLT/4LT rejection can be achieved by increasing the event logging rate to 1 kHz and using the cuts listed above along with a track impact parameter requirement similar to that used by SELEX. This assumption may be conservative, as *HERA-B*'s 4LT processor farm is more powerful than the SGI Challenge machine used by SELEX.

## 4 Acceptance and Efficiencies

We use a Monte Carlo (MC) sample of  $D^{*+} \rightarrow D^0 \pi^+$ ,  $D^0 \rightarrow K^- \pi^+$  decays to calculate the geometric acceptance and the efficiencies of the cuts used to obtain minimum bias rejection factors of 20 (FLT) and 6.3 (SLT). We run the standard *HERA-B* reconstruction package on these events to fill the RSEG and RTRA tables. We then calculate efficiencies in the reverse order in which the selection criteria would, in practice, be applied to the data: we first require that decays be fully-reconstructed (tracks in the RTRA table) and that they pass  $D^0$  and  $D^*$  mass requirements; we then require that events pass the SLT-level cuts; we then require that events pass the FLT-level cuts; and finally we require that events pass the pretrigger cuts. The first selection yields the reconstruction efficiency; the second selection yields the relevant SLT efficiency; the third selection yields the relevant FLT efficiency; and the last selection yields the relevant pretrigger efficiency. The product of all the factors yields the overall efficiency. When an additional efficiency factor is needed (e.g., the efficiency of the SLT impact parameter cut taken from SELEX), this factor is added by hand.

### 4.1 Reconstruction Efficiency

Some MTRA quantities exhibiting characteristics of  $D^*$  production and decay are plotted in Figs. 3-4. Fig. 3 shows the momentum spectrum of the  $K^-$  from the  $D^0$  (top), the  $\pi^+$  from the  $D^0$  (middle), and the  $\pi^+$  from the  $D^{*+}$ , respectively. The latter is denoted “ $\pi$  slow” or  $\pi_s$  to distinguish it from the  $\pi^+$  from the  $D^0$  decay. Fig. 4 shows the corresponding



	$N$	Fraction	
		relative	absolute
Events generated	10000		
Number $D^{*+} \rightarrow D^0 \pi^+$ , $D^0 \rightarrow K^- \pi^+$ decays	12671	1.	1.
$K^-$ track reconstructed (in RTRA)	3988	0.315	0.399
$\pi^+$ track reconstructed (in RTRA)	1488	0.373	0.149
$\pi_s$ segment reconstructed (in RSEG)	1176	0.790	0.118
$ m_{K\pi} - m_{D^0}  < 60 \text{ MeV}/c^2$	1030	0.876	0.103
$10.0 < p_{rat} < 19.0$	978	0.950	0.098
$p_{dot} < 0.32$	888	0.908	0.089

Table 2: The number of Monte Carlo  $D^{*+} \rightarrow D^0 \pi^+$ ,  $D^0 \rightarrow K^- \pi^+$  decays reconstructed and passing analysis cuts. The final result (8.88%) is taken as the reconstruction efficiency.

$p_T$  spectra. We note that the  $\pi_s$  has low momentum and very low  $p_T$ . These characteristics are due to the fact that there is little kinetic energy released in the decay  $D^{*+} \rightarrow D^0 \pi^+$ ; in fact the  $p_T$  of the  $\pi_s$  is essentially that of the parent  $D^{*+}$ .

We use the MTRA  $\rightarrow$  RSEG  $\rightarrow$  RTRA links to find RTRA tracks corresponding to the  $K^-$  and  $\pi^+$  daughters. If these are found, we compare  $p_z$  ( $z$  component of momentum) as listed in RTRA with that listed in MTRA. We treat the  $\pi_s$  from  $D^{*+} \rightarrow D^0 \pi^+$  differently, as this MTRA usually does not have a reconstructed RTRA. However, the MTRA usually has an RSEG in the PC region, and we propagate or “swim” this RSEG upstream through the magnet to the position of the target wires ( $z = 0$ ) using the routine `rgauxsmv` written by A. Spiridonov. The reconstructed momentum for the  $\pi_s$  is taken to be the upstream value returned by `rgauxsmv`.

Using RTRA momenta we calculate  $m_{K\pi}$ ,  $p_{rat}$ , and  $p_{dot}$  and make the selection cuts listed in Table 2. This table also gives the resulting efficiencies. The fraction of events in which the  $D^0 \rightarrow K^- \pi^+$  is reconstructed and  $|m_{K\pi} - m_{D^0}| < 60 \text{ MeV}/c^2$  is 10.3%; the fraction of these events that pass the nominal  $p_{rat}$  cut is 95%; and the fraction of these that pass the nominal  $p_{dot}$  cut is 91%. The overall reconstruction efficiency is 8.88%.

Fig. 5 shows the  $m_{K\pi}$ ,  $p_{rat}$ , and  $p_{dot}$  distributions for signal MC events, calculated using RTRA quantities. The events entering each plot have passed the previous requirements in the order listed in Table 2. The distributions are very similar to the corresponding ones obtained using MTRA momenta and confirm that one can reliably cut on these quantities. Also shown (top right) is the mass spectrum when the pion and kaon tracks are purposely misidentified; during actual analysis this “wrong-mass” will be calculated and the event rejected if it is near  $m_{D^0}$ , in order to reject background from Cabibbo-favored  $D^0 \rightarrow K^- \pi^+$  decays. The figure shows that the corresponding efficiency loss for signal events will be very small.

## 4.2 SLT/4LT Efficiency

To calculate the SLT/4LT efficiency, we consider events passing the above reconstruction requirements and impose the SLT/4LT-level requirements studied with the minimum bias

sample. Most of these requirements are in fact the same as those applied to reconstruct events. We thus need only consider the efficiency of extra cuts, and there was one: that the swum  $x$  and  $y$  positions of the RSEG corresponding to  $\pi_s$  be within 18 cm of  $(0, 0)$ . The efficiency of this cut is listed in Table 3; the value is 0.97.

As discussed previously, it is assumed that the SLT/4LT will need to make a track impact parameter cut similar to that made by SELEX to achieve the requisite rejection factor of 50 (for an event logging rate of 1 kHz). We thus adopt SELEX’s efficiency of 50% for lack of a better value. Finally, we assume an SLT tracking efficiency of 0.90 per track. The overall SLT/4LT efficiency is thus  $0.97 \times 0.50 \times (0.90)^3 = 0.35$ .

### 4.3 FLT Efficiency

For the FLT to find the  $K^-$ ,  $\pi^+$ , and  $\pi_s$  tracks, they must traverse a sufficient number of ITR and/or OTR chambers. We thus require that the  $\pi^+$  and  $\pi_s$  tracks be accepted by all four PC stations (either ITR or OTR); in this case the FLT would use tracks seeds from either PC4 or PC1. The former has the advantage that it would presumably be the “quietest” chamber, while the latter has the advantage that it is closest to the PT3 station and thus would have the smallest FLT region-of-interest (used by the FLT to initiate a track search). For the  $K^-$  we require that the track be accepted by TC1; this ensures that the track traverses the RICH, whose information is needed to distinguish between doubly-Cabibbo-suppressed  $D^0 \rightarrow K^+\pi^-$  signal events and Cabibbo-favored  $D^0 \rightarrow K^-\pi^+$  background events as misidentifying the tracks still often gives a two-body mass close to  $m_{D^0}$ . From MC simulation we obtain the results listed in Table 3. Requiring that all three tracks be accepted by the four PC chambers and that the  $K^-$  track also be accepted by TC1 gives a geometric acceptance of 58.3%.

Due to the way the analysis code is written, this number is now combined with the geometric acceptance of the HPT pretrigger chambers. For the high- $p_T$  system to determine the track seeds, all three tracks must traverse either all three inner HPT chambers or all three outer HPT chambers; i.e., the pretrigger coincidence boards process hits from the two systems separately. From MC simulation this acceptance is found to be 60.6%.

For events in which all three tracks are accepted by the PC/TC1 and HPT chambers, we find the corresponding RSEGs in the PC chambers and calculate the momenta using Eq. 2. The values obtained are found to approximate the momenta giving in the RTRA table to reasonable accuracy (see Figs. X). We use these momenta to calculate  $p_{asym}$ ,  $m_{K\pi}$ ,  $p_{rat}$ , and  $p_{dot}$  and require that they satisfy the same FLT-level requirements used to obtain the minimum-bias rejection factor of 20, i.e.:

- momentum asymmetry:  $|p_A - p_B| / (p_A + p_B) < 0.70$ .
- invariant mass:  $1.820 < m_{K\pi} < 2.010 \text{ GeV}/c^2$ .
- momentum ratio:  $10 < (p_{z(1)} + p_{z(2)}) / p_{z(3)} < 19 \text{ GeV}/c$ .
- momentum dot-product:  $P_3 \cdot (P_1 + P_2) < 0.32$ .

The individual efficiencies are listed in Table 3; the combined efficiency is 67.1%. We multiply this by the collective efficiency of the tracking chambers, optical links, and TFU/TPU/TDU

	$N$	Fraction	
		relative	absolute
Reconstructed $D^{*+} \rightarrow D^0 \pi^+$ , $D^0 \rightarrow K^- \pi^+$ (Table 2)	888		
$\pi_s$ $ x_{swm}  < 18$ cm, $ y_{swm}  < 18$ cm	861	0.970	1.0
$K^-$ track accepted by PC1-PC4 and TC1	632	0.734	
$\pi^+$ track accepted by PC1-PC4	681	0.791	
$\pi_s$ track accepted by PC1-PC4	839	0.974	
<b>all 3 tracks accepted (FLT tracking)</b>	<b>502</b>	<b>0.583</b>	<b>0.583</b>
$K^-$ track accepted by inner or outer HPT1–3	466	0.928	
$\pi^+$ track accepted by inner or outer HPT1–3	458	0.912	
$\pi_s$ track accepted by inner or outer HPT1–3	351	0.699	
<b>all 3 tracks accepted (HPT pretrigger)</b>	<b>304</b>	<b>0.606</b>	<b>0.353</b>
RSEGs satisfy $ p_{asym}  < 0.70$	281	0.924	0.326
$1.820 < m_{K\pi} < 2.010$ GeV/ $c^2$	225	0.801	0.261
$10 < p_{rat} < 19$	214	0.951	0.249
$p_{dot} < 0.32$	204	0.953	0.237

Table 3: The number of Monte Carlo  $D^{*+} \rightarrow D^0 \pi^+$ ,  $D^0 \rightarrow K^- \pi^+$  decays satisfying SLT (top) and FLT (bottom) trigger requirements.

boards, which is estimated [13] to be 0.7 per track. Finally, we include an additional efficiency factor to account for the fact that the trigger may need to require hits in both PC2 and PC3 stations, which are single-layer chambers. Since the chamber efficiency is 0.95 per layer, this factor is  $(0.95)^6 = 0.74$ . Thus, the overall FLT efficiency is taken to be  $0.583 \times 0.606 \times 0.671 \times (0.70)^3 \times 0.74 = 0.060$ . This number includes the acceptance of the HPT chambers.

Fig. 6 shows the  $p_{asym}$ ,  $m_{K\pi}$ ,  $p_{rat}$ , and  $p_{dot}$  distributions for signal MC events, calculated using RSEG (PC) quantities. The events entering each plot have passed the previous requirements in the order listed in Table 3. Note that the range selected for  $m_{K\pi}$  is asymmetric with respect to  $m_{D^0}$ .

#### 4.4 Pretrigger Efficiency

The geometric acceptance of the HPT chambers was already included in the FLT efficiency calculated above. The results are given in Table 3. However, we must also include the chamber efficiencies and the efficiency of the optical links and pretrigger logic. The former is estimated to be  $(0.95)^9 = 0.63$ , while the latter is estimated to be 0.50. These additional factors total  $0.63 \times 0.50 = 0.32$ .

Fig. 7 displays the HPT geometric acceptance in a graphical format. In these histograms, bins 1–3 have entries for tracks accepted by the inner PT1, inner PT2, and inner PT3 chambers, respectively. Bins 5–7 have entries for tracks accepted by the outer PT1, outer PT2, and outer PT3 chambers, respectively. From these plots we observe that:

- the  $K^-$  and  $\pi^+$  tracks traverse the inner region more often on average than the outer

region; the ratio is approximately 3:2. If the tracks traverse the first HPT station, they usually traverse the last two HPT stations.

- the  $\pi_s$  track traverses the inner PT1 station more often than the inner PT2 or inner PT3 stations, but it traverses the outer PT3 station more often than the outer PT2 or outer PT1 stations. This behavior reflects the fact that the  $\pi_s$  usually has low momentum and thus significant curvature away from the beam as it traverses the magnet.

## 5 Estimate of Sample Size

We estimate the sample size as follows. Details of the various terms entering this calculation have been discussed in previous sections.

We assume a nominal interaction rate of 1.0 MHz and a ratio of production cross sections

$$R = \frac{\sigma(pN \rightarrow D^{*+}X)}{\sigma(pp)_{inel}} = 4.7 \times 10^{-3}.$$

This ratio is calculated as follows: the cross section  $\sigma(pN \rightarrow D^{*+}X)$  is taken from Andrej Gorisek's thesis [14] to be  $158 \pm 63^{+25}_{-32}$   $\mu\text{b}/\text{nucleon}$ , and the inelastic cross section  $\sigma(pp)_{inel}$  is taken as the difference between  $\sigma(pp)_{tot}$  and  $\sigma(pp)_{elastic}$ . These cross sections are listed by the Particle Data Group [15, 16] to be  $\sigma_{tot} = 41$   $\text{mb}/\text{nucleon}$  and  $\sigma_{elastic} = 7.4$   $\text{mb}/\text{nucleon}$  for  $p_p = 1000$   $\text{GeV}/c \approx p_{HERA}$ . Thus  $\sigma_{inelas} = 33.6$   $\text{mb}/\text{nucleon}$  and  $R = 4.7 \times 10^{-3}$ . Since  $\sigma_{D^*}$  scales approximately linearly with atomic number  $A$ , and  $\sigma_{inelas}$  scales approximately as  $A^{2/3}$ , we must scale  $R$  by a factor  $A^{1/3}$  to account for different target materials. For a tungsten target,  $A = 184$ ,  $A^{1/3} = 5.69$ , and thus  $R_W = 0.027$ . The branching fractions  $B(D^{*+} \rightarrow D^0\pi^+)$  and  $B(D^0 \rightarrow K^-\pi^+)$  are 0.683 and 0.0385, respectively [15], and multiplying these factors by  $R_W$  and the nominal interaction rate gives a total production rate of 703 Hz.

We now use the various efficiency factors calculated in the previous sections: a geometric acceptance + reconstruction efficiency of 0.0888, an SLT efficiency of 0.35, an FLT efficiency of 0.060, and a pretrigger efficiency of 0.32. We also include an efficiency factor of 0.20 to account for additional offline analysis cuts. Multiplying all factors together gives a total trigger, reconstruction, and analysis efficiency of  $1.2 \times 10^{-4}$ . Multiplying this by the production rate gives 0.084 Hz, or, assuming  $10^7$  live seconds per year (30% duty cycle),  $8.4 \times 10^5$  reconstructed  $D^0 \rightarrow K^-\pi^+$  decays per year. We rescale this factor by the ratio of branching fractions to obtain the yields of  $D^0 \rightarrow K^+K^-$ ,  $D^0 \rightarrow \pi^+\pi^-$ , and DCS  $D^0 \rightarrow K^+\pi^-$  decays listed in Table 4. We estimate that *HERA-B* would reconstruct about 3000  $D^0 \rightarrow K^+\pi^-$  decays per year, or 6000 decays in two years of running. This is a very large sample. The experiment would also reconstruct about 180 000 SCS  $D^0 \rightarrow K^+K^-$  decays and 60 000 SCS  $D^0 \rightarrow \pi^+\pi^-$  decays in two years. We note that *CP* violation may occur with different strengths in these three modes. In addition, a very large sample of Cabibbo-favored  $D^0 \rightarrow K^-\pi^+$  decays would be reconstructed for calibration purposes and efficiency studies.

Mode	Branching fraction (%)	Estimated <i>HERA-B</i> yield (2 years)	Estimated BaBar yield (350 fb <sup>-1</sup> )
$D^0 \rightarrow K^- \pi^+$	3.85	$1.7 \times 10^6$	$1.02 \times 10^6$
$D^0 \rightarrow K^+ K^-$	0.412	180 000	100 000
$D^0 \rightarrow \pi^+ \pi^-$	0.143	63 000	49 000
$D^0 \rightarrow K^+ \pi^-$	0.0138	6 000	1920

Table 4: Estimated event yields in  $2 \times 10^7$  s of running. The right-most column lists the corresponding events yields expected for BaBar in 350 fb<sup>-1</sup> of data (2005). Note that the BaBar yield for  $D^0 \rightarrow K^+ \pi^-$  is reduced relative to the other modes due to tighter analysis cuts.

For comparison, the BaBar experiment has reconstructed  $26084 \times (97\% \text{ purity}) = 25300$   $D^0 \rightarrow K^+ K^-$  decays and  $12849 \times (88\% \text{ purity}) = 11300$   $D^0 \rightarrow \pi^+ \pi^-$  decays in 91 fb<sup>-1</sup> of data [4], and  $430 \times (73\% \text{ purity}) = 314$   $D^0 \rightarrow K^+ \pi^-$  decays in 57.1 fb<sup>-1</sup> of data [7]. BaBar has thus far (summer 2003) recorded 131 fb<sup>-1</sup> of data [17] and is expected to record roughly 350 fb<sup>-1</sup> by summer 2005. Rescaling these event yields by the ratio of luminosities gives the expected BaBar samples also listed in Table 4. The Belle experiment is expected to reconstruct similar amounts. Comparing these yields to the *HERA-B* yields in two years of running ( $2 \times 10^7$  s) shows the latter to be very competitive and possibly larger. Given the large *HERA-B* sample sizes, and the very good lifetime resolution of the *HERA-B* detector, we expect the experiment to have high sensitivity to *CP* violation and mixing.

## 6 Estimate of Sensitivity

We obtain a first estimate of the precision with which the mixing parameters  $x'$  and  $y'$  could be measured using the  $D^0 \rightarrow K^+ \pi^-$  sample via a toy Monte Carlo study. We generate  $D^0 \rightarrow K^+ \pi^-$  decays according to the lifetime distribution given by Eq. (1), smear the events by the lifetime resolution, and then do an unbinned maximum-likelihood fit for  $x'$  or  $y'$ . The point where the negative-log-likelihood function is minimized is taken as the central value, and the points where the negative-log-likelihood function has risen by 0.5 is taken as the  $1\sigma$  errors. In fact a two-dimensional unbinned fit should be performed, as done in Ref. [7]; here we do only 1-d fits for expediency. Nonetheless, the fits allow us to compare the precision *HERA-B* could attain with those that Belle/BaBar would attain.

We must add an appropriate level of background to the sample. For *HERA-B* we assume a nominal lifetime cut of  $0.87\tau_D$  will be made in the offline analysis, and that the resulting signal-to-background ratio will be 0.20. This ratio is similar to the background level observed by FNAL E791 in their search for  $D^0$ - $\bar{D}^0$  mixing using  $D^{*+} \rightarrow D^0 \pi^+$  decays [5]. (This experiment produced  $D^{(*)}$  mesons via  $\pi N$  collisions with a similar center-of-mass energy as that of *HERA-B*, and had similar geometric acceptance as that of *HERA-B*). Thus when doing our fits we include only events having  $t > 0.87\tau_{D^0}$ , and for this range of lifetime we add five times as many background events to the sample as signal events. As the dominant source of background observed by E791 (and also Belle/BaBar) is random

Generated $x'^2$ ( $\times 10^{-3}$ )	Fit result for <i>HERA-B</i> sample	Fit result for BaBar sample
0.4	$0.67 \pm 0.08$	$0.33^{+0.11}_{-0.10}$
0.6	$0.80 \pm 0.08$	$0.51^{+0.13}_{-0.12}$
0.8	$0.93^{+0.10}_{-0.09}$	$0.70^{+0.15}_{-0.14}$
1.0	$1.06 \pm 0.10$	$0.89^{+0.17}_{-0.15}$
1.2	$1.19 \pm 0.11$	$1.09^{+0.17}_{-0.16}$
1.4	$1.35^{+0.12}_{-0.11}$	$1.31 \pm 0.18$

Table 5: Results of the unbinned maximum likelihood fit for  $x'$  for the nominal *HERA-B* (left) and BaBar samples (right). The parameters  $\tau = 411.7$  fs and  $y' = 0$ .

combinations of Cabibbo-favored  $D^0 \rightarrow K^- \pi^+$  decays with spurious pions originating from the primary vertex, we generate the background events with a decay-time dependence of  $e^{t/\tau_D}$ .

The lifetime resolution  $\sigma$  used for smearing is dominated by the  $z$  resolution of the  $D^0$  decay vertex. We take this value to be  $700 \mu\text{m}$  and approximate the lifetime resolution by multiplying this value by  $m_{D^0}/(c \cdot \langle p \rangle)$ , where  $m_{D^0}$  and  $p$  are in  $\text{GeV}/c^2$  and  $\text{GeV}/c$ , respectively. For  $\langle p \rangle = 36 \text{ GeV}/c$  (obtained from the MC acceptance study), we obtain  $\delta\tau \approx 121$  fs. This is better than Belle/BaBar’s  $D^0 \rightarrow K^- \pi^+$  lifetime resolution of 200 fs [18, 7].

When fitting for  $x'$  and  $y'$ , we fix the parameter  $R$ , which is the ratio of the branching fractions for  $D^0 \rightarrow K^+ \pi^-$  to  $D^0 \rightarrow K^- \pi^+$ . For this value we use the recent BaBar result  $R = 3.59 \times 10^{-3}$  [7], and we fix the  $D^0$  lifetime to the PDG value of 411.7 fs. For simplicity we assume no  $CP$  violation. In fact we fit for  $x'^2$  rather than  $x'$ , as the pdf (Eq. 1) depends on this parameter only quadratically. Our results for the  $x'^2$  fit for  $y' = 0$  are listed in Table 5. Also listed are the results for a corresponding “BaBar sample:” we assume a sample size of 1920 events, no lifetime cut, a signal-to-background ratio of 3, and a lifetime resolution of 220 fs. These latter values are taken from Ref. [7]. The table shows that the statistical errors obtained with the *HERA-B* fit are uniformly smaller than the errors obtained with the BaBar fits. We find similar behavior when fitting for the parameter  $y'$ . In Fig. 8 we show the generated and smeared signal samples, and the total sample with background, for “data” generated with  $x'^2 = 0.0006$ . Fig. 9 shows the corresponding distributions for the BaBar fit. Fig. 10 shows the likelihood function resulting from the *HERA-B* fit, and Fig. 11 shows the likelihood function from the BaBar fit.

## 7 R & D Effort

Given the favorable sample sizes obtained above, we propose to proceed with R & D to develop a  $D^{*+} \rightarrow D^0 \pi^+$  trigger. This effort would proceed in several steps:

1. Detailed simulation of the  $D^{*+} \rightarrow D^0 \pi^+$  trigger algorithm ( $p_{asym}$ ,  $m_{K\pi}$ ,  $p_{rat}$ , and  $p_{dot}$  cuts) at the trigger board level.

2. Design and build a prototype TDU board that could trigger on 3 tracks, i.e., execute the  $p_{asym}$ ,  $m_{K\pi}$ ,  $p_{rat}$ , and  $p_{dot}$  requirements.
3. Install the new TDU in the FLT and test.
4. Transfer some of the optical links, trigger-link boards, and TFU's from the TC1/TC2 chambers to PC2/PC3, reprogram the TFU's to reconstruct tracks using information only from the PC chambers, and take test data with beam. Such operation also requires programming the message boards of the HPT pretrigger system to send message words to the FLT.

These steps require different amounts of effort. The first three steps are not large, while the last step is a substantial project. Clearly it would only be undertaken if the preceding steps were successful.

The first step, detailed simulation of the  $D^{*+} \rightarrow D^0\pi^+$  trigger algorithm, would refine the studies presented here. The Monte Carlo acceptance study for signal events would be repeated with a bit-level simulation of the pretrigger and FLT hardware. Using the number of bits available and the coding schemes for the kinematic track parameters (momentum and position at PC1), the resolution of the bit-level calculation of the hardware can be calculated. This will subsequently determine the true efficiency and rejection power of the trigger algorithm. The kinematic variables used to calculate invariant mass,  $p_{rat}$ ,  $p_{dot}$ , etc., are themselves calculated by the TDU in several steps. Thus, intermediate results need to be stored with a certain precision. The interplay between a possible hardware implementation and the resulting simulated performance will guide the design of the TDU. The simulation work would also provide an estimate of the latency of the board, which can influence the design.

The second step, design and construction of a new TDU board, would probably be undertaken by the Mannheim group. This group designed and built the original TFU's, TPU's and TDU for *HERA-B* and has expressed some interest in this new project.

The third step is relatively straightforward: the new TDU would be installed in the FLT and tested by loading messages into the TPU output and processing them through the TDU.

The fourth step requires much work: some number of optical links and TFU's would need to be transferred from the TC chambers to PC2 and PC3. This would require a couple of weeks of effort working in the experimental area. Technician support would greatly facilitate this work. The number of planes of PC2 and PC3 that would be cabled and input to the FLT for sufficient rejection needs to be studied: possibly only one or both of the  $0^\circ$  projection layers would be needed. These layers are doubled and thus, or-ing them together, they would provide higher hit efficiency ( $1 - 0.05^2$ ) than the other layers.

In parallel with this work, the message boards for the HPT system would need to be programmed and the HPT system brought up to functional form. This would require several weeks of effort by the HPT group (ITEP and Cincinnati). Finally, data with beam would be taken with parts of the *HERA-B* detector, specifically the TARGET, FLT, HPT, OTR, VDS, and DAQ systems. The detectors that would remain off are the ITR, MUON, and ECAL systems. This would require the efforts of approximately 20–25 people. To collect sufficient test data would probably require of order a couple of weeks of reliable detector

operation. Presumably this could be integrated into the HERA schedule in a parasitic manner.

The time scale required for these activities is very roughly as follows:

- bit-level simulation studies: 5 months
- design and fabrication of a new TDU: 10 months
- installation of the TDU and testing in FLT: 1 month
- moving optical links, HPT work, test of trigger with beam: 4 months

Several of these activities would proceed in parallel, and thus the overall time scale would be (if all goes well)  $\sim$  one year. The number of people required for the first three steps is modest: just several of the experts from *HERA-B* and the Universität Mannheim Lehrstuhl für Informatik V. The fourth step would require about two dozen people; we are now actively discussing the project with colleagues at DESY (members of *HERA-B*) and at other labs (FNAL) to recruit collaborators for this test – and if successful, a follow-on charm mixing/*CP* experiment.

## 8 Summary

In summary, the studies presented here indicate the following:

- The *HERA-B* detector can be used to collect large, competitive samples of tagged SCS  $D^0 \rightarrow K^+K^-$ ,  $D^0 \rightarrow \pi^+\pi^-$ , and DCS  $D^0 \rightarrow K^+\pi^-$  decays. For example, we estimate that the experiment could reconstruct 3000  $D^0 \rightarrow K^+\pi^-$  decays per year of running. This is to be compared with  $\sim$  2000 such decays recorded each by Belle and BaBar in  $350 \text{ fb}^{-1}$  of data, which corresponds to several years of running. The decay time dependence of these samples would be used to measure/constrain the  $D^0$ - $\overline{D}^0$  mixing parameters  $x$  and  $y$  and search for *CP* violation in the  $D^0$ - $\overline{D}^0$  system. CLEO-c cannot make the same measurements as their  $D^0$  mesons are essentially at rest, and it may be difficult for CDF/D0 to make these measurements due to the very good particle ID needed to distinguish  $D^0 \rightarrow K^+K^-/\pi^+\pi^-/K^+\pi^-$  decays from the more copious (Cabibbo-favored)  $D^0 \rightarrow K^-\pi^+$  decays.
- The statistical errors obtained for  $x'$  and  $y'$  may be substantially smaller than the current errors on these quantities [7].
- The sensitivity to mixing may be comparable to theoretical predictions [12, 19]; i.e., the experiment may *observe* mixing. Knowledge of mixing in the  $D^0$ - $\overline{D}^0$  system could be very important for correctly extracting the CKM angle  $\phi_3/\gamma$  from  $B^\pm \rightarrow DK^\pm$  decays [12].
- The statistical errors for a signal-to-background ratio of  $\sim$  5 would be similar to (and possibly smaller than) those obtained by the Belle and BaBar experiments by 2005. The systematic errors will be different.

However, three technical hurdles need to be overcome in order to run the experiment:



1. a new TDU (Trigger Decision Unit) module for the FLT would need to be built that can select three-track combinations satisfying the  $p_{rat}$  and  $p_{dot}$  requirements. Mannheim has expressed interest in designing and building this unit.
2. the event logging rate must be increased from its current rate of  $\sim 200$  Hz to a rate of  $\sim 1000$  Hz.
3. an inner tracker is needed in the PC region (only) than can be used for triggering. Clearly this is a substantial construction project, but it may be well-matched to the interests and capabilities of new collaborators. It may be possible to use the existing inner tracker chambers with new electronics.

There are in fact some simplifications of the proposed experiment with respect to *HERA-B*: the MUON and ECAL detectors and corresponding triggers are not needed for the measurement; the FLT regions-of-interest would be very small, as they would be based on extrapolation only from the HPT chambers to the PC region; and the experiment would run at an interaction rate of only 1 MHz. It is worth noting that a large fraction of work required to mount an experiment involves software development, both online and offline. For a new experiment in the West Hall, much of *HERA-B*'s software can be re-used or serve as a template.

At the present time we propose to initiate R&D work to address the first technical hurdle and establish the  $D^{*+} \rightarrow D^0 \pi^+$  trigger concept. If the successful operation of such a trigger is proved, then the case can be made to proceed with a state-of-the-art charm mixing/ $CP$  violation experiment.

## References

- [1] E. M. Aitala *et al.*, Phys. Rev. Lett. 83, 32 (1999).
- [2] J. M. Link *et al.* (FOCUS Collaboration), Phys. Lett. B485, 62 (2000).
- [3] K. Abe *et al.* (BELLE Collaboration), BELLE-CONF-347, hep-ex/0308034 (2003).
- [4] B. Aubert *et al.* (BaBar Collaboration), Phys. Rev. Lett. 91, 121801 (2003); hep-ex/0306003.
- [5] E. Aitala *et al.* (E791 Collaboration), Phys. Rev. D57, 13 (1998).
- [6] R. Godang *et al.* (CLEO Collaboration), Phys. Rev. Lett. 84, 5038 (2000).
- [7] B. Aubert *et al.* (BaBar Collaboration), hep-ex/0304007 (2003).
- [8] B. Yabsley, private communication.
- [9] J. M. Link *et al.* (FOCUS Collaboration), Phys. Rev. Lett. 86, 2955 (2001).
- [10] <http://www-cdf.fnal.gov/>.
- [11] <http://www.lns.cornell.edu/public/CLE0/spoke/CLE0c/index.html>.
- [12] S. Bianco, F. L. Fabbri, D. Benson, and I. Bigi, hep-ex/0309021 (2003), pp. 143–162.
- [13] B. Schwingenheuer, private communication.

- [14] A. Gorišek, “Cross Section Measurement of  $D^0$  and  $D^{*+}$  Meson Production in Inelastic Collisions of 920 GeV Protons with Nuclei,” Ph.D. thesis, University of Ljubljana, Slovenia (2002).
- [15] K. Hagiwara *et al.* (Particle Data Group), Phys. Rev. D66, 010001 (2002).
- [16] <http://pdg.lbl.gov/xsect/contents.html>.
- [17] [http://www.slac.stanford.edu/BFROOT/www/Detector/  
Operations/babar\\_integrated.gif](http://www.slac.stanford.edu/BFROOT/www/Detector/Operations/babar_integrated.gif).
- [18] K. Abe *et al.* (Belle Collaboration), hep-ex/0308034 (2003).
- [19] I.I. Bigi and N.G. Uraltsev, Phys. Rev. B592, 92 (2001).

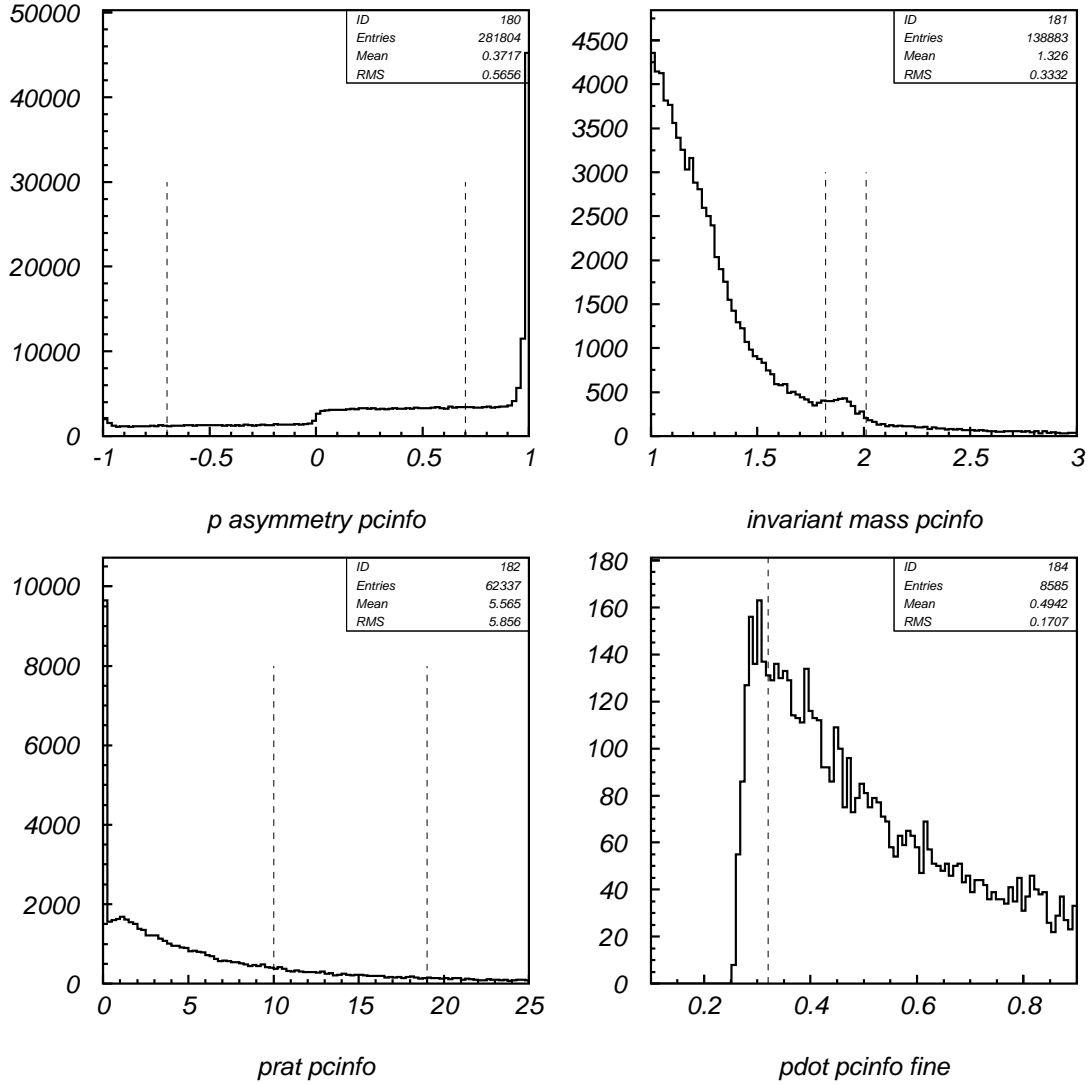


Figure 2: Distributions of  $p_{asym}$ ,  $m_{K\pi}$ ,  $p_{rat}$ , and  $p_{dot}$  for minimum bias events, calculated using only PC (RSEG) information. The dashed vertical lines denote the selected ranges.

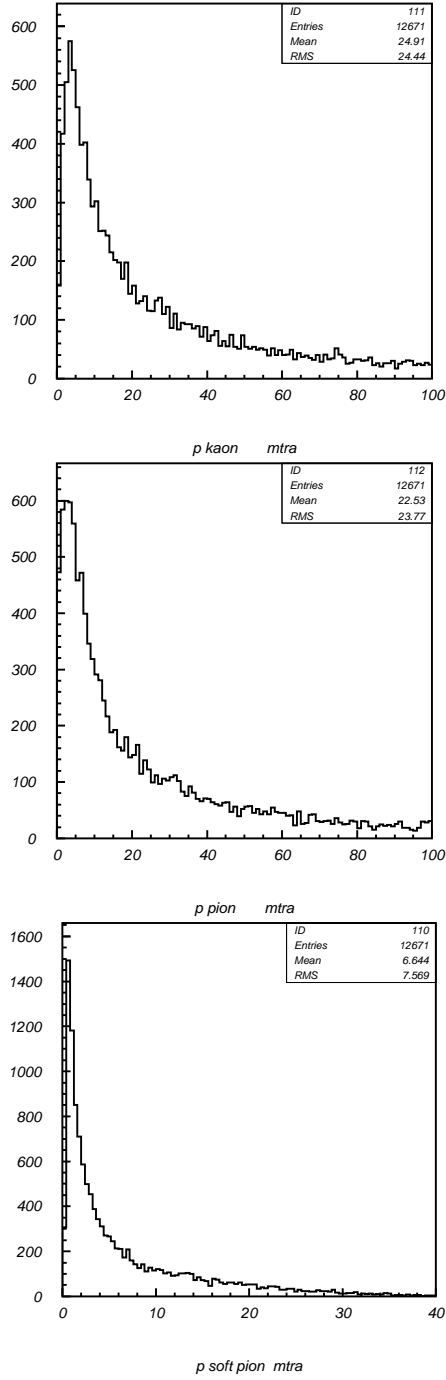


Figure 3: The momentum spectra of the  $K^-$  from the  $D^0$  (top); the  $\pi^+$  from the  $D^0$  (middle); and the  $\pi_s$  from the  $D^{*+}$  (bottom).

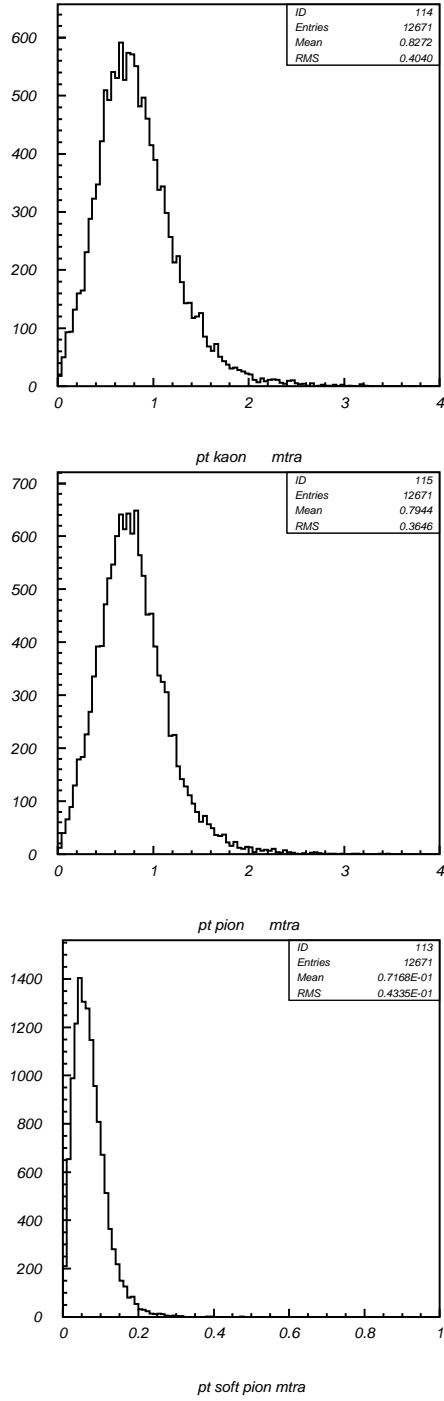


Figure 4: The  $p_T$  spectra of the  $K^-$  from the  $D^0$  (top); the  $\pi^+$  from the  $D^0$  (middle); and the  $\pi_s$  from the  $D^{*+}$  (bottom).

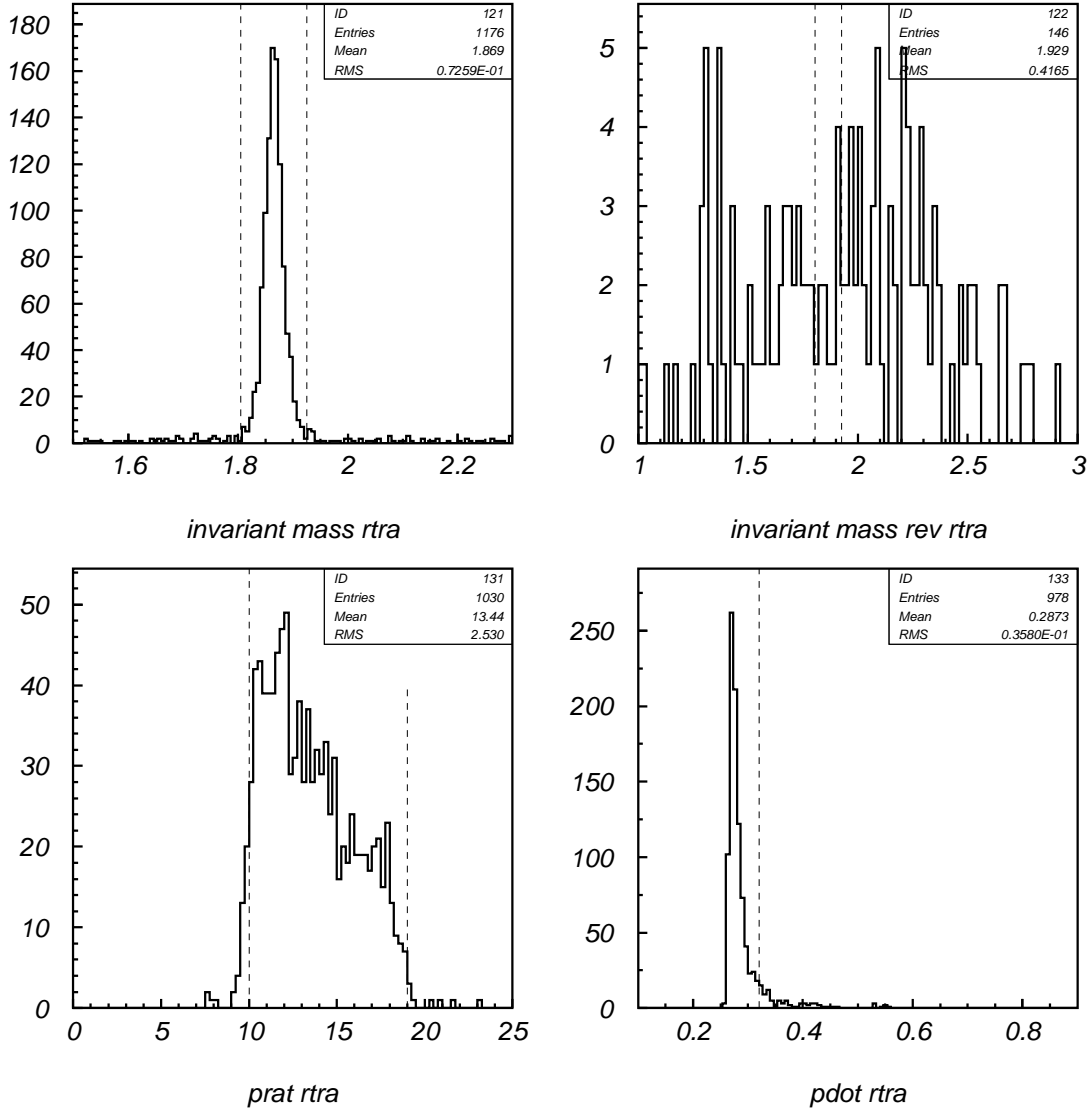


Figure 5: Distributions of  $m_{K\pi}$ ,  $m_{wrong}$  (see text),  $p_{rat}$ , and  $p_{dot}$  for Monte Carlo  $D^{*+} \rightarrow D^0 \pi^+$ ,  $D^0 \rightarrow K^- \pi^+$  decays, calculated using RTRA information. The dashed vertical lines denote the selected ranges.

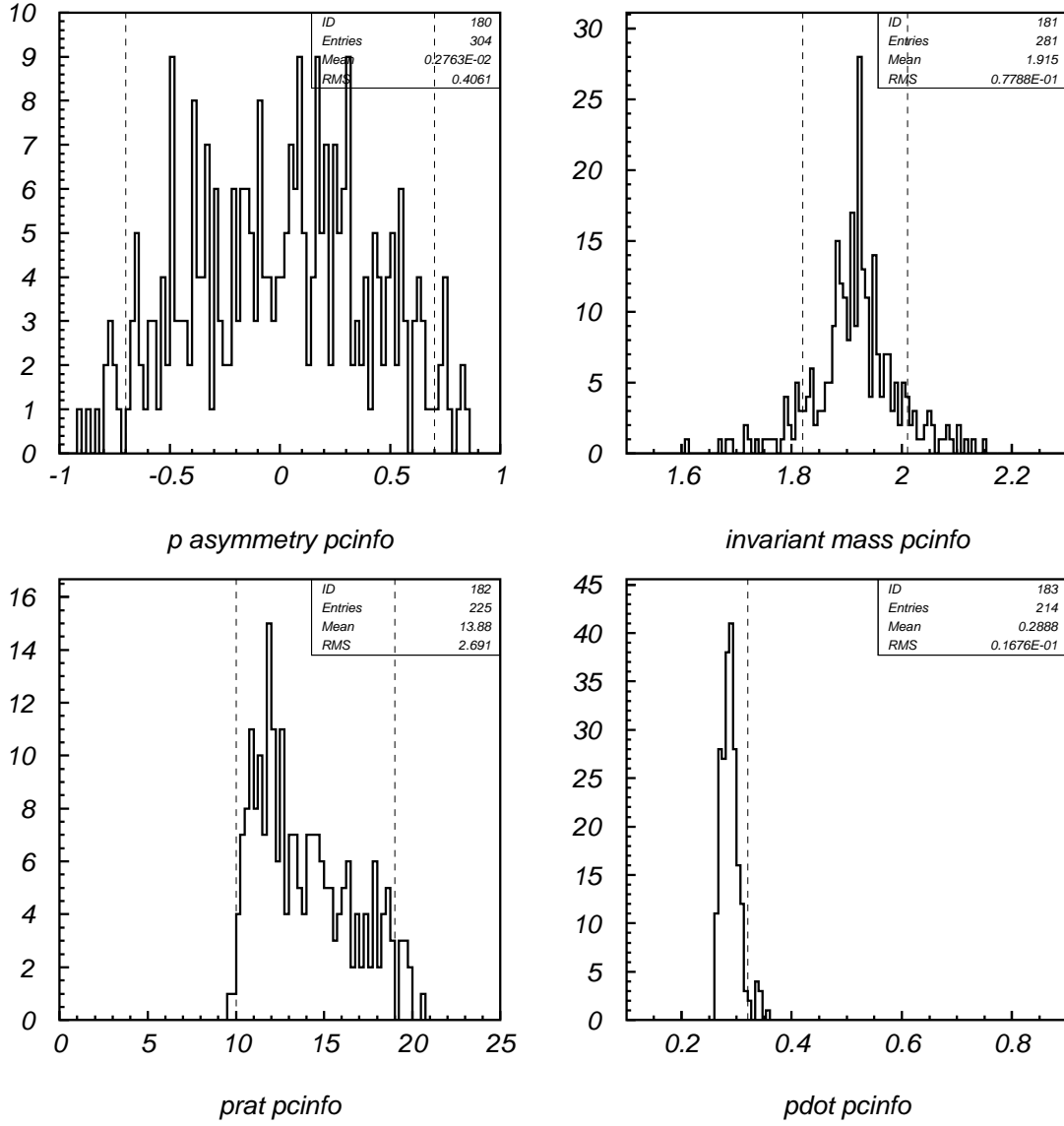


Figure 6: Distributions of  $p_{asym}$ ,  $m_{K\pi}$ ,  $p_{rat}$ , and  $p_{dot}$  for Monte Carlo  $D^{*+} \rightarrow D^0 \pi^+$ ,  $D^0 \rightarrow K^- \pi^+$  decays, calculated using PC (RSEG) information. The dashed vertical lines denote the selected ranges.

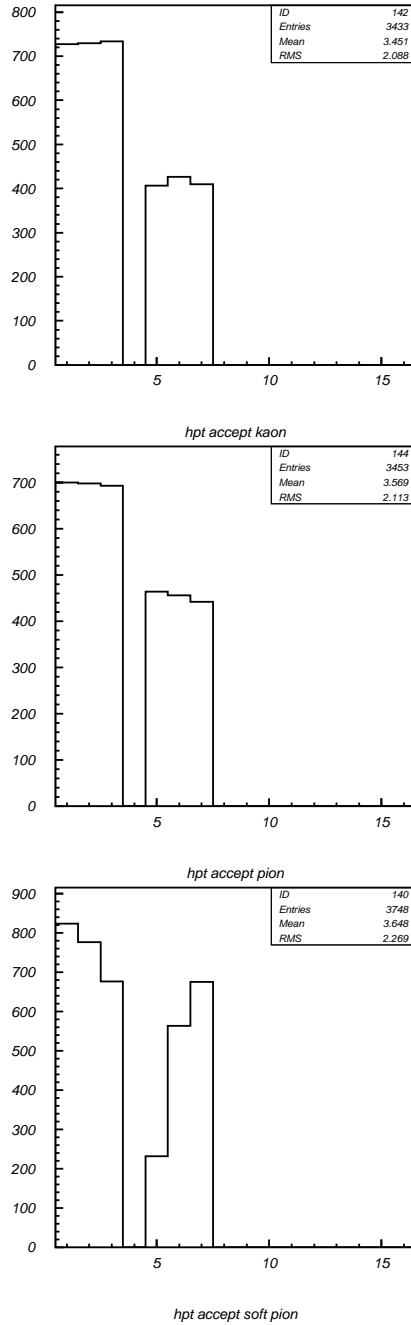


Figure 7: The acceptance of the HPT chambers for the  $K^-$  track (top), the  $\pi^+$  track (middle), and the  $\pi_s$  track (bottom). Bins 1–3 correspond to inner PT1, inner PT2, and inner PT3, respectively; bins 5–7 correspond to outer PT1, outer PT2, and outer PT3, respectively (see text).



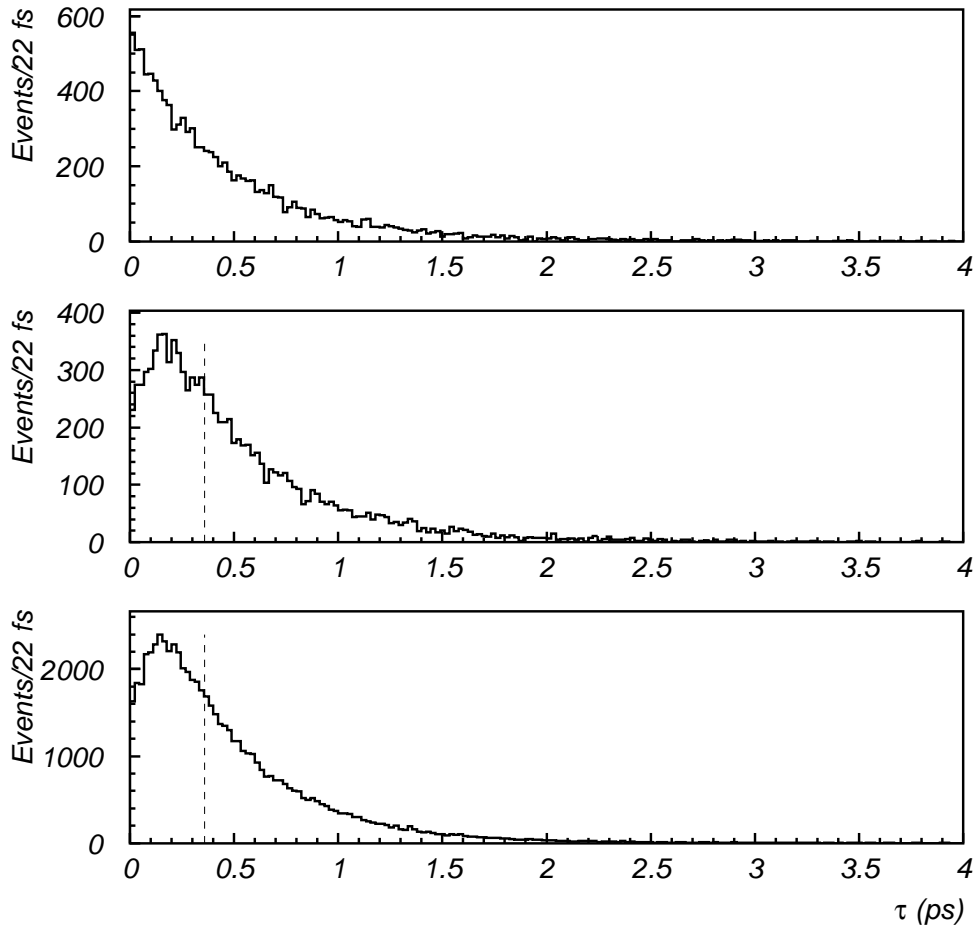


Figure 8: The distribution of generated signal events (top) for  $x'^2 = 0.0006$ ,  $y' = 0$ ; after smearing by a lifetime resolution of 120 fs (middle); and after being combined with a smeared background sample five times larger. The dashed vertical line indicates the lifetime cut (to reject background) used in the study.

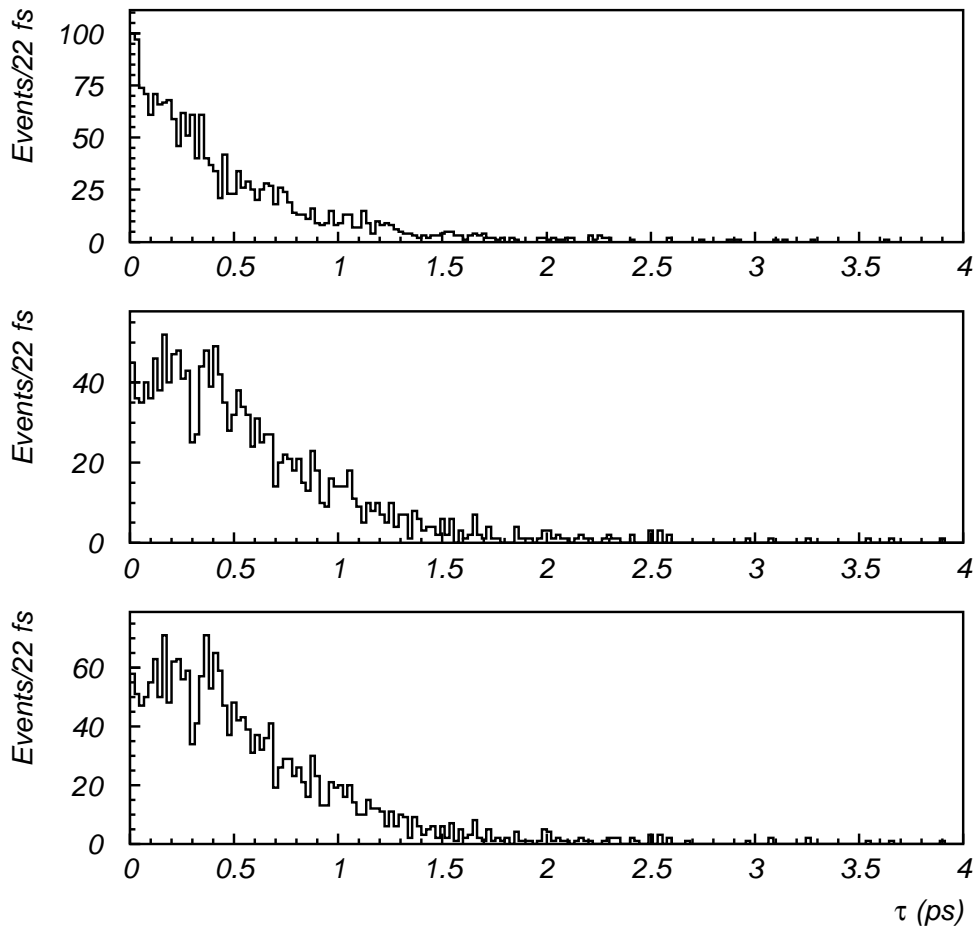


Figure 9: The distribution of generated signal events (top) for  $x'^2 = 0.0006$ ,  $y' = 0$ ; after smearing by a lifetime resolution of 220 fs (middle); and after being combined with a smeared background sample 1/3 as large.

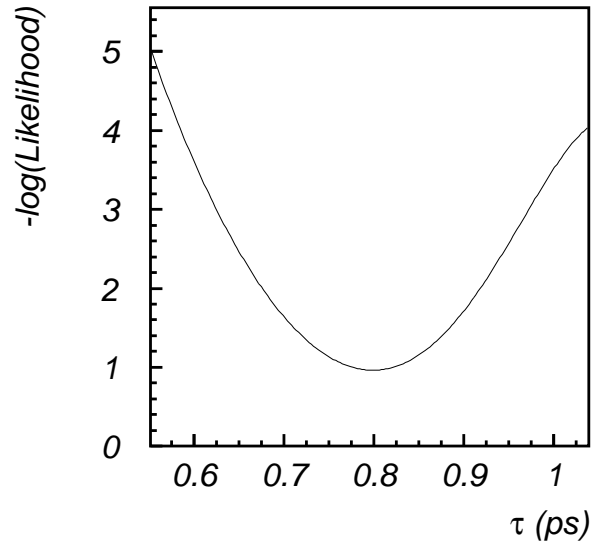


Figure 10: The likelihood function resulting from the “HERA-*B* fit,” for  $x'^2 = 0.0006$  and  $y' = 0$ .

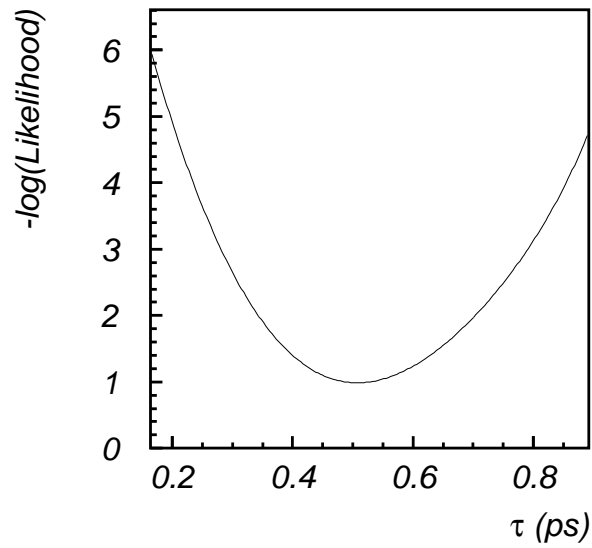


Figure 11: The likelihood function resulting from the “BaBar fit,” for  $x'^2 = 0.0006$  and  $y' = 0$ .